



Effect of processing variables on efficiency of eucalyptus pulps for internal curing

Passarin Jongvisuttisun^a, Camille Negrello^{a,b}, Kimberly E. Kurtis^{a,*}

^a School of Civil and Environmental Engineering, Georgia Institute of Technology, 790 Atlantic Dr., Atlanta, GA 30332-0355, USA

^b Civil Engineering Department, Ecole Normale Supérieure de Cachan, 94235 Cachan Cedex, France

ARTICLE INFO

Article history:

Received 9 August 2012

Received in revised form 16 November 2012

Accepted 20 November 2012

Available online 29 November 2012

Keywords:

Autogenous shrinkage

Cellulose

Fiber reinforcement

Wood-derived fibers

Water entrainment

ABSTRACT

This study evaluates the effect of fiber composition and morphology, as altered by various papermaking processes, on internal curing performance of hardwood eucalyptus pulp fibers. The autogenous deformations of cement pastes containing each of five different eucalyptus pulps—unbleached soda pulp, bleached soda pulp, unbleached kraft pulp, bleached kraft pulp, and semi-chemical pulp—were examined and analyzed in the context of the known relevant chemical composition and morphology, e.g., cellulose-to-hemicellulose ratio, cell wall thickness, and “hard to remove” (HR) water content. The results revealed that the internal curing efficiency of these pulps is related more strongly to their physical morphology than chemical composition, as measured by cellulose-to-hemicellulose ratio. The partial defiberization during mechanical treatment associated with semi-chemical pulping resulted in fiber fracture and also produced materials which were poorly dispersible; together, these factors limit internal curing capability of semi-chemical pulp. The soda fibers, both unbleached and bleached, with their thicker cell wall and higher HR water content were more effective for internal curing than kraft fibers. It is proposed that for hardwood pulp fibers a slower rate of entrained water release is beneficial for internal curing.

© 2012 Elsevier Ltd. All rights reserved.

1. Introduction

The use of saturated lightweight aggregates and superabsorbent polymers (SAPs) as internal curing agents for the prevention of self-desiccation in high-performance concrete (HPC) has been examined because both materials can gradually release water to the surrounding hydrating paste [1–5]. Further, research has elucidated the key mechanisms controlling the effectiveness of both saturated lightweight aggregates and SAPs for this application. For saturated lightweight aggregates, capillary suction has been shown to be an important mechanism of water transport from the relatively larger pores in saturated lightweight aggregates to the surrounding and more finely porous cement paste, with vapor diffusion and capillary condensation also playing a role in moisture transport [6,7]. The key mechanisms controlling the internal curing capacity of SAPs are the combination of the swelling ratio, ion filtration, and the inter-particle spacing of the SAPs [6,8,9].

Cellulose or pulp fibers have also been studied as an alternative to saturated lightweight aggregates and SAPs for internal curing. These renewable materials have been shown to not only have the capacity to substantially reduce autogenous shrinkage but also to provide additional resistance to shrinkage-induced cracking by increasing tensile capacity [10]. While the abilities of different

types of cellulose fibers (e.g., softwood thermomechanical pulp, softwood kraft pulp, and specialty cellulose fibers) to mitigate autogenous shrinkage in cement paste and mortar have been shown [10–12], the features of the fibers—both chemical and physical—affecting their efficacy as internal curing agents remain relatively unexplored. In particular, the influence of fiber pulping on the internal curing capacity of fibers is an important topic because even in the same type of wood, the morphology and composition of its pulp can be altered by processing, and these alterations could have significant effects on the ability of the fibers to limit autogenous shrinkage. Therefore, an improvement in the understanding of the relationship between fiber properties and internal curing efficacy would make the selection, dosing, and even design of pulp fiber for internal curing in mortar and concrete more precise. More fundamentally, improved knowledge of the relationships between fiber parameters and changes in autogenous shrinkage should provide new understanding of the mechanism(s) by which cellulosic materials function as internal curing agents.

In pulp fibers, water can be held in the fiber lumen (or cavity enclosed by the cellulose-rich cell wall) or bound to and within the cell wall itself. The maximum amount of free water which can be held in the lumen could be related to the size of the lumen and its structure (e.g., open, closed, collapsed), which are in turn related to the type of wood and the processing of the fiber such as pulping, drying history, and refining. For example, fibers which have been dried after pulping may have collapsed lumens, which may limit their use for internal curing. The capacity to bind water

* Corresponding author. Tel.: +1 (404) 385 0825; fax: +1 (404) 894 2278.

E-mail addresses: p.jongvisuttisun@gatech.edu (P. Jongvisuttisun), camille.negrello@ens-cachan.fr (C. Negrello), kimberly.kurtis@ce.gatech.edu (K.E. Kurtis).

is also dependent upon the chemical compositions of the pulp—cellulose, hemicellulose, and lignin contents—which affect the fiber's ability to attract and bind polar water molecules. Since pulp fibers are derived from various types of wood and various pulping processes impart different structural and chemical characteristics, fibers derived from different wood species or subjected to different pulping processes are expected to exhibit different internal curing capabilities. In prior research [11], the effects of chemical treatments on the internal curing performance of a species of softwood fibers from thermomechanical pulping (TMP) process were evaluated. Early hydration behaviors and autogenous shrinkage test results of chemically treated fibers—holocellulose TMP and α -cellulose TMP—cement pastes were compared to that of the ordinary TMP-cement paste. However, that investigation concluded that further information of fiber morphology was needed, along with the known relevant chemical composition, i.e. cellulose-to-hemicellulose ratio, to better understand these complex relationships. It is also not clear if the results obtained previously for softwood fibers would also be applicable to hardwood species, such as eucalyptus.

While native to Australia, eucalyptus is now grown in most parts of the world in tropical and subtropical climates (e.g., North and South America, Africa, Mediterranean, Middle East, and Southeast Asia) and is of considerable interest to researchers and environmentalists alike because of their fast growth rate, which makes them highly renewable. Recently, Tonoli et al. [13] demonstrated the advantages of eucalyptus pulps as a reinforcement of cementitious materials; these include their high dispersibility and effective crack bridging. However, the internal curing performance of eucalyptus pulps had not been examined in their or other studies.

This present work evaluates the effect of variations in processing conditions of hardwood *Eucalyptus camaldulensis* fibers to produce five fibers—unbleached soda pulp, bleached soda pulp, unbleached kraft pulp, bleached kraft pulp, and semi-chemical pulp—and their performance as internal curing agents. The structure and composition of five different fiber variants were first evaluated by image analysis and thermal analysis techniques. Each of these fibers results from different processing of the same hardwood eucalyptus species. Then, the internal curing capacities of the fibers measured through standard autogenous shrinkage testing are compared to fiber composition and morphology, to better clarify the complex roles these factors play in providing internal curing to cement-based materials.

2. Materials and methods

2.1. Materials

Eucalyptus camaldulensis (or River Red gum) fibers, sourced from Southeast Asia, were evaluated in this study. Fibers from five common commercial treatments, varying the types of chemicals used and the use of mechanical action during treatment—unbleached soda pulp (USF), bleached soda pulp (BSF), unbleached kraft pulp (UKF), bleached kraft pulp (BKF), and semi-chemical pulp (SCF)—were collected from commercial papermaking processes. The effect of internal restraint was evaluated by comparing the autogenous shrinkage test results of pulp fiber–cement pastes with that of the polypropylene fiber–cement paste (Grace MicroFiber™), chopped to approximately 0.5–1.5 mm in length (e.g., approximately the same length as the pulp fibers) to isolate the influence of the internal curing from any internal restraint provided by the fibers. The diameter of the polypropylene fiber was approximately 20–25 μm , which is slightly larger than the hardwood pulp fibers, but reasonably similar.

The fiber–cement samples tested in this study by calorimetry and autogenous shrinkage experiments were prepared by mixing the as-received, never dried, fibers with ASTM Type I/II portland cement (Lafarge, North America) and deionized water (DI water, resistivity of 18.2 $\text{M}\Omega\text{ cm}$) at a fixed w/c of 0.30. The oxide analysis was performed by X-ray fluorescence (XRF, Bruker AXS S8 Tiger) spectrometry. The oxide composition of the cement is (percentage by mass): 19.73% SiO_2 , 4.82% Al_2O_3 , 3.16% Fe_2O_3 , 62.41% CaO , 3.64% MgO , 2.99% SO_3 , 0.08% Na_2O , 0.48% K_2O , and LOI of 2.2%. The crystalline phases of cement were determined by performing quantitative X-ray diffraction analysis (QXRD, Bruker AXS D4 Endeavor) with the Rietveld method using TOPAS software. The crystalline phase composition of the cement is (percentage by mass): 52.6% alite, 20.7% belite, 3.7% aluminate, 11% ferrite, 0.1% lime, 2.3% portlandite, 2.6% periclase, 0.6% arcanite, 0.4% aphtthitalite, 0.9% gypsum, 2.4% bassanite and calcite of 2.7%.

2.2. Image analysis to quantify morphology of eucalyptus pulp fibers

The cross-sectional dimensions of eucalyptus fibers were assessed by performing image analysis on scanning electron micrographs. Fiber morphological properties can be quantified effectively based on statistical image analysis with microscopy techniques [14,15]. Samples for each of the fibers were dispersed in DI water, vacuum filtered at $74.5 \pm 3.5\text{ kPa}$ ($22 \pm 1\text{ in Hg}$), and freeze-dried in order to eliminate clumping of the fibers, to prevent collapse of the fiber ultra-structures, and to preserve their microstructure. Freeze-dried fiber bundles were embedded in a hydrophilic aromatic acrylic resin (LR white embedding medium) and heat cured in a convention oven at $60\text{ }^\circ\text{C}$ for 24 h. After the acrylic resin was polymerized, samples were ground using silicon carbide paper with a grit size of 320, 600, and 1200, and polished using a 1.0 and 0.3 μm of aluminum oxide powder. Images of polished samples were acquired with a Hitachi S-3700N variable pressure scanning electron microscope at $600\times$ magnification with a 20 kV accelerated voltage and 9–10 mm of working distance. Using the public-domain, Java-based image processing program ImageJ, gray-scale images were thresholded and converted to binary images, as shown in Fig. 1. In the binary image, small particles, such as grinding debris and other fine materials, and split fibers were discarded. Then, the modal values of the diameters of the fiber and lumen in the fitted data were determined based on a statistical analysis of 350 cross-sectional fiber images per fiber type.

2.3. Composition and hard-to-remove water analysis of eucalyptus pulp fibers

The compositions of the five fiber types were determined through measurements of lignin content, cellulose-to-hemicellulose ratio, and hard-to-remove (HR) water content. The lignin content in fibers was determined by a kappa number test according to TAPPI Standard T236. The total residual lignin content (TRLCL) were calculated according to $\text{TRLCL} = \text{kappa number}/6.546$ [16]. Because the kappa numbers of bleached pulp were very small, the residual lignin content in both bleached fibers was assumed to be insignificant, as expected for this type of fiber processing. The ratio of cellulose-to-hemicellulose of each fiber was determined by measuring the weight change of samples during thermogravimetric analysis. As-received fibers were dried at $23 \pm 2\text{ }^\circ\text{C}$ and $42 \pm 3\%\text{RH}$ in a ventilation hood for 24 h prior to the test. Samples were placed in a thermogravimetric analyzer (TGA), TA instrument Q5000IR. The nitrogen gas flow rate was 20 mL/min for both balance and sample chamber gas. Samples were heated up from room temperature to $600\text{ }^\circ\text{C}$ at a constant heating rate of $10\text{ }^\circ\text{C}/\text{min}$. Since the main decomposition temperature of hemicellulose and cellulose occurs mainly at $220\text{--}315\text{ }^\circ\text{C}$ and $315\text{--}400\text{ }^\circ\text{C}$,

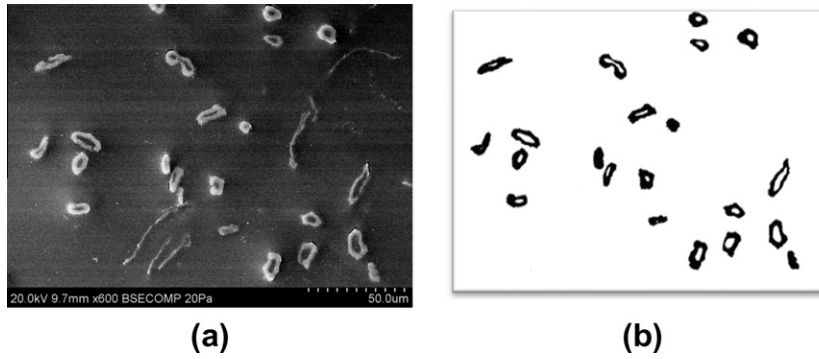


Fig. 1. Typical cross-section of fibers embedded in an acrylic resin (a) gray-scale SEM image and (b) binary image for analysis.

respectively [17], the cellulose-to-hemicellulose ratio of the fibers was defined as the fraction of the percent weight change at 315–400 °C to the percent weight change at 220–315 °C.

In addition, for the purpose of understanding the use of pulp fibers for internal curing, it is important that relative availability of moisture provided by the fiber be assessed by measuring the HR water content. HR water can be defined as the moisture ratio (grams of water per gram of dry fiber) at the transition between the constant and the falling rate zones of evaporative changes in mass detected by during TGA [18]. Park et al. [18] proposed that the amount of HR water could be used as an indicator of the range in moisture content within which moisture loss from the fibers is controlled by internal diffusion. Therefore, this research will relate HR water to both fiber properties (e.g., fiber type, pore volume, and fiber wall thickness) and fiber–cement pastes properties, such as autogenous and chemical shrinkage. TGA was used to determine the HR water content in each fiber. The nitrogen gas flow rate was 20 mL/min for balance and sample chamber gas. Measurements of change in mass were made under isothermal conditions at 50 °C until the weight change was negligible. The resolution of the instrument was 0.001 µg.

2.4. Fiber quality analysis

Fiber Quality Analyzer (FQA) was used to characterize the arithmetic mean length (\bar{L}_n), the weight-weighted mean length (\bar{L}_w), the fiber coarseness, and the length-weighted percent fines content for each pulp fiber. FQA is a widely used optical fiber analyzer that gathers information of fibers through projected images of the fibers in a dilute suspension transported through the optical and imaging systems. Since the mass of dry fiber (f), the total number of fiber (n), and the number of fiber in the length class l_i (n_i) were known, the \bar{L}_n and \bar{L}_w , could be calculated as follows:

$$\bar{L}_n = \sum n_i l_i / n \quad (1)$$

$$\bar{L}_w = \sum n_i l_i^3 / \sum n_i l_i^2 \quad (2)$$

Coarseness of the fiber is the “weight of fiber wall material in a specified fiber length” [19]. From FQA data, the mean value of fiber coarseness was:

$$\text{Fiber coarseness (mg/m)} = f \times 1000 / \bar{L}_n \times n \quad (3)$$

The length-weighted percent fines content was calculated by dividing the total length of measureable fines (0.07–0.10 mm in length) by the total length of measureable fines and fibers. The maximum length of fine fraction set in this experiment was 0.1 mm.

2.5. Autogenous deformation

The mix proportions for the control and fiber–cement paste samples were selected to maintain a constant amount of “entrained” water (e.g., water available for internal curing) with the constant amount of cement (by weight) and the w/c of 0.30, 0.31, and 0.32, listed in Table 1. The amount of fiber added to the cement paste depended on the absorption capacity (k) of the fiber, as determined by the method described by Johansen et al. [20]. Based on the assumptions that internal curing agents will absorb water from the mix to equilibrate at k and that they neither accelerate nor slow the rate of hydration, the k of fibers can be calculated by comparing the early heat evolution data of the fiber–cement pastes to those of ordinary cement pastes at a similar w/c. Absorption of water by the internal curing agents would be expected to produce calorimetry curves similar to those for ordinary pastes at a lower w/c; thus, the amount of water absorbed can be used to calculate k for an internally cured paste of known composition.

To determine the k of fibers, fibers were first assumed to have k at 1. Then, using Eqs. (4) and (5), the mass of mixing water (M_W) and the mass of as-received fibers (M_F) were calculated based on the mass of cement proportioned for the mixture (M_{CEM}), the moisture content of each fiber (MC, determined according to ASTM D4442-07 [21]), the assumed k (k_A), and dry fiber mass-to-cement ratio (f/c). Then, the early heat evolution data of fiber–cement pastes were compared to those of ordinary cement pastes to determine the effective w/c (w/c_{eff}). Then, the k_A of fibers was adjusted to the actual k of the fibers (Eqs. (6) and (7)).

$$M_W = M_{CEM} \times \{w/c - [(MC/100 - k_A) \times f/c]\} \quad (4)$$

$$M_F = M_{CEM} \times f/c \times (1 + MC/100) \quad (5)$$

$$\Delta k = \frac{w/c - w/c_{eff}}{f/c} \quad (6)$$

$$k = k_A + \Delta k \quad (7)$$

The effectiveness of eucalyptus fibers as internal curing agents was examined through the comparison of autogenous shrinkage test results of fiber–cement pastes to those of the cement pastes at three different water-to-cement ratios, i.e. w/c = 0.30, 0.31, and 0.32. The autogenous deformation was measured according to ASTM C1698-09 [22]. After mixing, the pastes were cast and sealed in corrugated polyethylene tubes having an outer diameter of 29 ± 0.5 mm with a length of 420 ± 5 mm. All of the samples were stored in an environmental chamber at 25 ± 1 °C during the entire test period. When the pastes reached the final set, determined according to ASTM C191-08 [23], measurements of the

Table 1
Mix designs for the autogenous shrinkage measurements.

| | Control | | | Fiber–cement paste | | | | | | | | |
|---------------------------------------|---------|----------|----------|--------------------|--------|------------|--------|-----------|--------|-----------|--------|--------|
| | w/c 0.3 | w/c 0.31 | w/c 0.32 | USF | BSF | SCF | SCF 1% | UKF | UKF 1% | BKF | BKF 1% | PP 1% |
| As-received MC ^a (%) | – | – | – | 487 | 417 | 529 | 529 | 401 | 401 | 414 | 414 | – |
| <i>k</i> | – | – | – | 1 | 1 | 1.5 | 1.5 | 2 | 2 | 2 | 2 | – |
| Cement (g) | 1500 | 1500 | 1500 | 1500 | 1500 | 1500 | 1500 | 1500 | 1500 | 1500 | 1500 | 1500 |
| Water (g) | 450 | 465 | 480 | 391.95 | 402.45 | 412.10 | 393.15 | 434.93 | 419.85 | 433.95 | 417.90 | 450 |
| Dry fiber (g) | – | – | – | – | – | – | – | – | – | – | – | – |
| [Dry fiber-to-cement in mass percent] | – | – | – | 15 [1] | 15 [1] | 10 [0.667] | 15 [1] | 7.5 [0.5] | 15 [1] | 7.5 [0.5] | 15 [1] | 15 [1] |
| As-received fiber (g) | – | – | – | 88.05 | 77.55 | 62.90 | 94.35 | 37.58 | 75.15 | 38.55 | 77.10 | 15 |
| w/c | 0.3 | 0.31 | 0.32 | 0.3 | 0.3 | 0.3 | 0.3 | 0.3 | 0.3 | 0.3 | 0.3 | 0.3 |
| w _e /c ^b | – | – | – | 0.01 | 0.01 | 0.01 | 0.015 | 0.01 | 0.02 | 0.01 | 0.02 | – |

^a The moisture content of fibers is expressed as a percentage of the oven-dry mass of fibers.

^b The term w_e/c is the amount of entrained water to cement by mass.

initial deformation were taken. The test data of fiber–cement pastes were compared with that of the control sample, which contained no internal curing agent.

3. Results and discussion

To evaluate the internal curing performance of fibers, autogenous shrinkage experiments of cement pastes—w/c = 0.30, 0.31, and 0.32—and fiber–cement pastes were performed. For more understanding of factors controlling the internal curing capacity of eucalyptus fibers, the autogenous shrinkage test results were then evaluated and analyzed in the context of fiber properties.

3.1. Fiber properties

Table 2 summarizes results from the physical and chemical analysis of the fibers and provides data describing each fiber's diameter, the lumen diameter, the cell wall thickness, the fiber coarseness, the arithmetic mean fiber length, the weight-weighted mean fiber length, and the length-weight percent fines content, as well as other properties of each fiber, including *k*, the kappa number, the total residual lignin content, the cellulose-to-hemicellulose ratio, and the amount of HR water measured.

The frequency distributions of the fiber and lumen diameters obtained through the statistical image analysis previously described are shown in Figs. 2 and 3, respectively. By using OriginPro data analysis software, the discrete frequency distributions of the

fiber diameter were fitted based on Pearson IV distribution, while that of the lumen diameter were fitted based on log-normal distribution. Fitting parameters were iterated until the fit converged (Chi-square tolerance value of 1E-9 was reached). The modal values for the fiber diameter and lumen diameter can be determined from the peak values, evaluated by using local maximum peak finding method, from curves fitted to the discrete frequency distributions shown in Figs. 2 and 3, respectively. The cell-wall thickness is the difference between the modal value of the fiber diameter and lumen diameter divided by two.

The weight-weighted mean fiber lengths, measured by using FQA, were range from 0.68 to 0.78 mm. The weight-weighted mean fiber length is more commonly used in paper science, because it is more related to sheet properties than other mean lengths [24]. Although the diameter of fiber, the thickness of cell wall, the density of cell wall, and the cross-section of fiber affect the coarseness of fiber, Table 2 shows that, the cell-wall thicknesses evaluated by image analysis seem well correlated with coarseness values evaluated by using FQA. A fiber that has high coarseness value could be expected to have a thick fiber wall [25].

Overall, the morphological properties resulting from the analysis of the fiber, determined from the image analysis and FQA, agree with prior research outcomes. Paavilainen [26] reported that the properties of hardwood vary between 0.7–1.7 mm, 2.5–5 μm, and 15–40 μm for the fiber length, the cell wall thickness, and the fiber width, respectively. Specifically, the morphological characteristics of *Eucalyptus camaldulensis* pulps grown in northern India are a fiber length of 0.8 ± 0.21 mm, a fiber width of 15 ± 3.1 μm, a lumen

Table 2
Fiber properties.

| Fiber properties | Types of fibers | | | | |
|--|-----------------|------------------|--------------|------------------|--------------|
| | USF | BSF | UKF | BKF | SCF |
| <i>k</i> ^a | 1 | 1 | 2 | 2 | 1.5 |
| Kappa number | 20–22 | N/A ^e | 25 | N/A ^e | 150–160 |
| Lignin content (%) | 3–3.3 | N/A ^e | 3.82 | N/A ^e | 23–24.5 |
| Cellulose-to-hemicellulose ratio ^b | 3.99 | 5.89 | 3.01 | 4.49 | 1.05 |
| HR water content ^b (g/g dry fiber) | 1.44 ± 0.11 | 1.45 ± 0.01 | 1.30 ± 0.02 | 1.37 ± 0.09 | 1.76 ± 0.06 |
| Fiber diameter ^c (μm) | 12.914 | 12.524 | 12.602 | 12.797 | 14.124 |
| Lumen diameter ^c (μm) | 5.067 | 4.716 | 5.341 | 5.341 | 5.380 |
| Cell wall thickness ^c (μm) | 3.924 | 3.904 | 3.631 | 3.728 | 4.372 |
| Coarseness ^d (mg/m) | 0.065 | 0.064 | 0.059 | 0.062 | 0.119 |
| Arithmetic mean length ^d (mm) | 0.471 ± 0.01 | 0.463 ± 0.01 | 0.481 ± 0.01 | 0.481 ± 0.00 | 0.418 ± 0.00 |
| Weight-weighted mean length ^d (mm) | 0.690 ± 0.02 | 0.778 ± 0.09 | 0.734 ± 0.04 | 0.771 ± 0.05 | 0.684 ± 0.01 |
| Length-weighted percent fines content ^d (%) | 0.73 ± 0.00 | 0.77 ± 0.01 | 0.93 ± 0.05 | 0.88 ± 0.03 | 1.12 ± 0.03 |

^a *k* of fibers were determined by performing isothermal calorimetry tests.

^b Cellulose-to-hemicellulose ratio and HR water content of fibers were determined by measuring the weight change of samples in TGA.

^c Fiber morphological properties—fiber diameter, lumen diameter, and cell wall thickness—were evaluated by performing an image analysis.

^d Fiber qualities—coarseness, arithmetic mean length, weight-weighted mean length, and length-weighted percent fines content—were determined by using FQA.

^e The kappa numbers of bleached fibers were very small. Therefore, the residual lignin content in bleached fibers was assumed to be negligible.

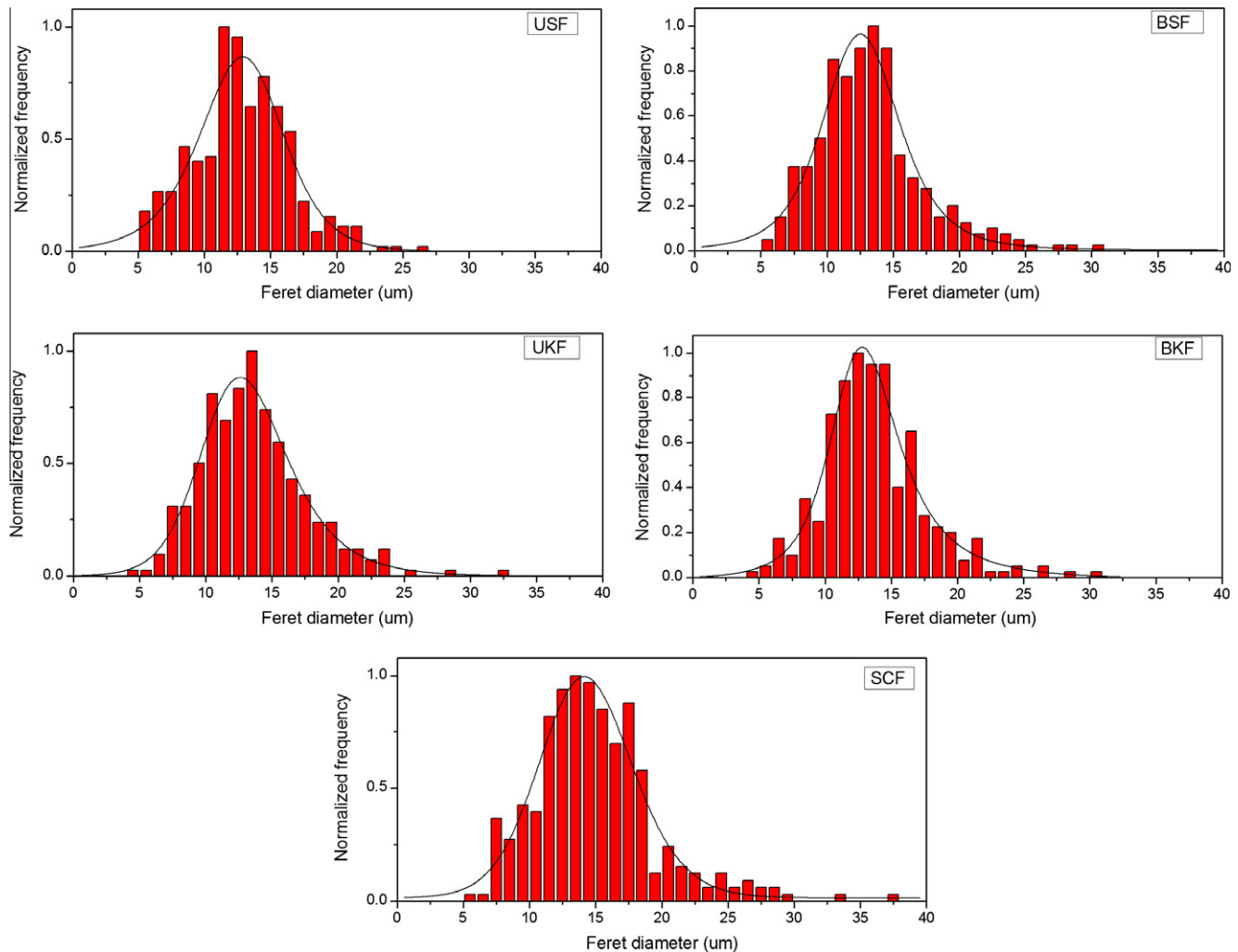


Fig. 2. Frequency distribution of the fiber diameters (μm) from the image analysis.

diameter of $7.2 \pm 0.8 \mu\text{m}$, and a cell wall thickness of $4.0 \pm 0.9 \mu\text{m}$ [27].

Among these fibers, it is worth noting the variation in chemical composition, particularly cellulose-to-hemicellulose ratio and lignin content. With regard to chemical composition, as expected, the lignin and hemicellulose content in the fiber decreased as the degree of chemical treatment increased. Both full chemically-treated fibers (BSF, BKF) had relatively high cellulose and low lignin contents compared to their corresponding unbleached fibers (USF, UKF), resulting in cellulose-to-hemicellulose ratios of approximately 4.5–6 and 3–4 of, respectively. In addition, due to its lowest level of chemical treatment (a mild chemical treatment followed by moderate mechanical refining) among five fibers tested, the SCF had the highest amount of both lignin and hemicellulose.

Fibers also vary in length-weighted percent fines content. Both soda fibers (USF, BSF) had the lowest fines content, while SCF had the highest, likely due to the mechanical aspects associated with this form of processing which are absent in the other soda and kraft processing methods. Some variation in k was also noted. Both soda fibers (USF, BSF) had k of 1 while that of SCF and both kraft fibers (UKF, BKF) were 1.5 and 2, respectively. This can be implied that, based on dry fiber mass, the soda fibers, SCF, and kraft fibers absorb water about 1, 1.5, and 2 times their own weight, respectively. Of the parameters measured, k seems most well-linked to the lumen diameter, with the larger k found for fibers with the

larger lumens. In addition, kraft fibers had a higher k of 2 perhaps because these fibers are characterized by a narrower cell wall thickness and a larger lumen diameter than soda fibers, with k of 1. These results coincide well with prior studies that found that the water retention value (WRV), the amount of water held in the fiber, determined by centrifuge method, decreased as the mean fiber wall thickness increased [28]. Since water is retained by capillarity inside the lumen, fibers with a thinner wall thickness and larger lumen diameter contain more water that could result in a higher k .

The fibers also varied in their proportion of HR water. While the SCF had the highest amount of HR water, the UKF had the lowest amount. While there is no clear relationship between the measured k and the HR water content, variations in the fiber morphology and composition may influence the amount of HR water measured. Since the HR water is a combination of both bound water and some amount of free water that located in small pores and capillaries, making it difficult to remove from fiber in the drying process, internal diffusion is considered to be the key mechanism for removal of HR water. Internal diffusion, then, depends on properties such as lumen diameter and volume, fiber wall thickness, fiber wall composition, and moisture content [29]. Therefore, both a smaller lumen diameter resulting in greater capillary tension and a thicker cell wall obstructing the diffusion of water to the surface contribute to a higher amount of HR water. From Table 2, a thicker cell wall thickness of soda fibers appears to

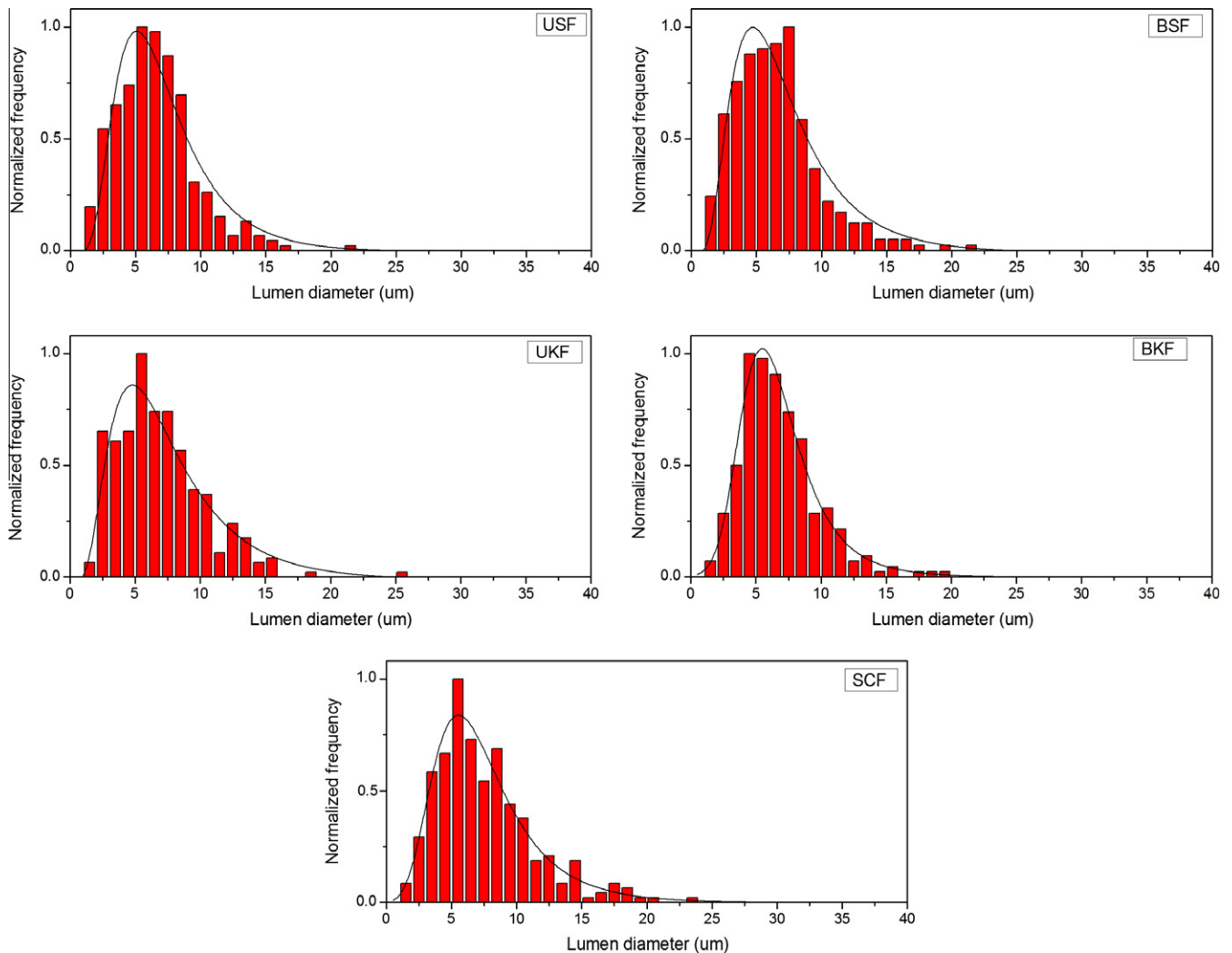


Fig. 3. Frequency distribution of the lumen diameters (μm) from the image analysis.

correspond with the higher amount of HR water. In addition to the thickness of the cell wall, the higher HR content in the SCF could also be related to the higher lignin content. Since the lignin (and some hemicellulose) removal results in increased fiber wall porosity [30,31]. Therefore, the higher lignin content in SCF could be interpreted that the cell wall of SCF is denser than other fiber types resulting in the slower moisture diffusion to the fiber surface.

3.2. Effect of fibers on early age hydration

Fig. 4 presents the effects of the incorporation of fiber on the rate of the hydration of cement paste assessed by isothermal calorimetry. The mix design (i.e., water contents) of the fiber–cement pastes were adjusted corresponding to k of each fiber (Table 2). With these adjustments, the addition of the fibers to the cement paste did not greatly affect the hydration rate of cement, as expected since the moisture expected to be absorbed by each fiber was accounted for in the mix design. Although the inclusion of BSF and BKF delayed the onset of the C_3S hydration peak by 20–40 min, respectively, the cumulative heat of hydration over the first 40 h did not vary much among the pastes (Fig. 5). By 50–60 h, the overall hydration of the fiber–cement pastes was slightly higher ($\sim 2\text{--}5\%$ at 60 h) than that of the control mix ($w/c = 0.30$), providing some evidence that the internal curing offered by the fibers promotes early cement hydration.

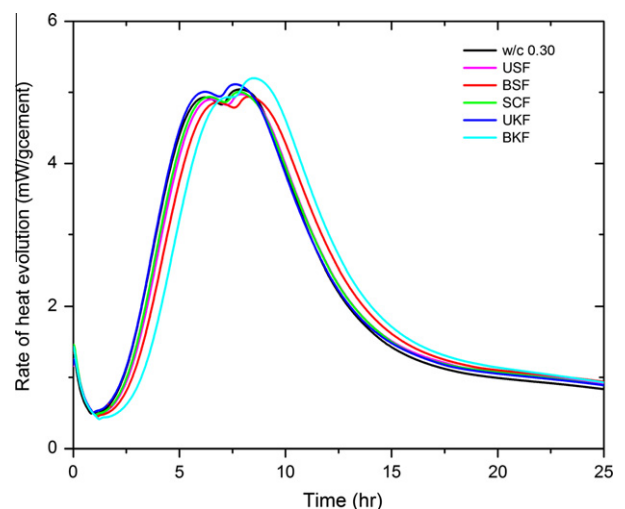


Fig. 4. Heat released from the cement paste compared with that of the fiber–cement pastes.

Accounting for only k , the preliminary results suggest that of the five eucalyptus variants examined kraft fibers and SCF are most advantageous for internal curing. However, a more comprehensive

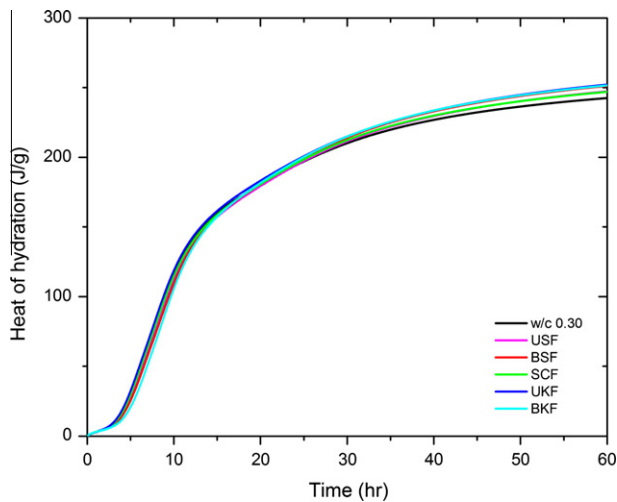


Fig. 5. Cumulative energy released from the cement paste compared with that of the fiber-cement pastes.

assessment of the potential of these fibers as internal curing agents necessitate further data pertaining to composition and morphology as well as measurements of early age deformation, as will be discussed subsequently.

3.3. Setting time and autogenous shrinkage behaviors of fiber-cement pastes

The capacities of the fibers to offset autogenous shrinkage by internal curing were compared through measurements of deformation made after the final set. The final set times of fiber-cement pastes, which were prepared to contain 0.01 of entrained water per gram of cement (based upon each fiber's determined k at a fixed w/c of 0.30), are compared to those of the cement pastes at $w/c = 0.30$ and 0.31 in Fig. 6. Although lignin derivatives such as lignosulfonate could retard the hydration reaction of calcium silicate phases [32], the use of fiber containing a high amount of lignin such as SCF (nearly 23% lignin) did not extend the time to set. Instead, the setting times determined by using Vicat apparatus were generally the same. The exception is BKF, which extended the time to set by 40 min. This fiber also resulted in some offsets in the rate of hydration data obtained in isothermal calorimetry. Together, this provides evidence that the fiber has some effect on slowing early hydration. However, as seen in Fig. 6, even BKF did not delay final set to the extent observed when increasing the

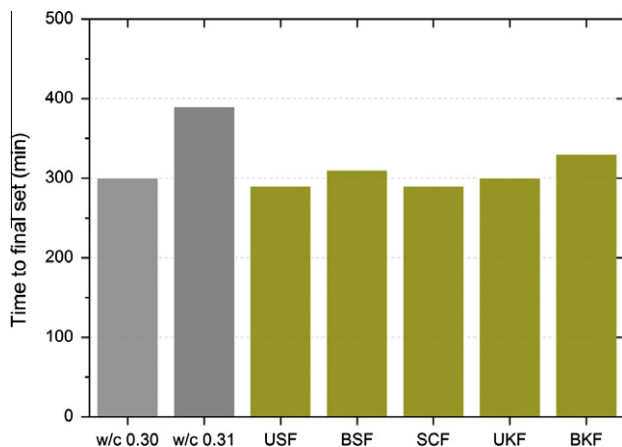


Fig. 6. Final setting time of the cement pastes compared with that of the fiber-cement pastes at 0.01 of entrained water.

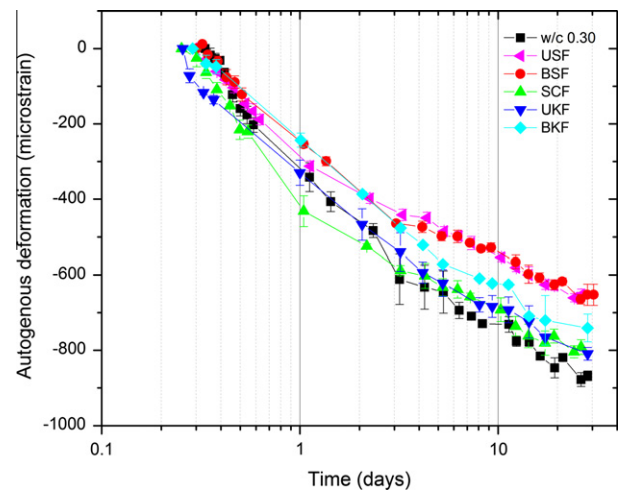


Fig. 7. Autogenous deformation of the cement paste compared with that of the fiber-cement pastes with 0.01 of entrained water.

w/c from 0.30 to 0.31, demonstrating that variations in setting time with the addition of eucalyptus fibers is minimal.

Fig. 7 compares the autogenous shrinkage of the cement paste and internally cured fiber-cement pastes, measured after the final setting. All of the fiber-cement pastes, shown in Fig. 7, were prepared based on the determined k of the fibers; each contains w_e/c of 0.01. Within the first few hours after the final setting, the fiber-cement pastes exhibited a slightly higher (or more negative) autogenous strain than cement paste, indicating either greater shrinkage or perhaps less bleeding during this period [33]. Over time, the rates of the shrinkage of the fiber-cement paste specimens were lower than that of the cement paste at w/c of 0.30. This indicates that the fibers, also in a paste with w/c of 0.30, released water into the hydrating cement and reduced self-desiccation.

At about 28 days, the fiber-cement pastes exhibited autogenous strain of $-652.05 \pm 14.73 \mu\epsilon$, $-652.58 \pm 28.25 \mu\epsilon$, $-791.52 \pm 19.84 \mu\epsilon$, $-809.09 \pm 16.85 \mu\epsilon$, and $-740.81 \pm 36.88 \mu\epsilon$ for the USF, BSF, SCF, UKF, and BKF, respectively, whereas cement paste at w/c of 0.30 underwent autogenous strain of about $-867.77 \pm 12.96 \mu\epsilon$. Examining the absolute deformation at 2 days shows that both kraft fibers and SCF, containing the same amount of entrained water as soda fibers, did not exhibit effective shrinkage reduction compared to the control paste (at w/c of 0.30). This can be taken to imply that reaching desirable internal curing efficiency requires higher dosage rates of the kraft fibers and SCF. It is also interesting in Fig. 7 to note that the effectiveness of BKF to mitigate autogenous shrinkage decreases with time, suggesting that entrained water was perhaps released too early with this fiber.

Overall, these results show that of the treatments of eucalyptus camaldulensis examined here, both types of soda fibers with the lowest k values of 1 were most effective at limiting autogenous shrinkage, with a $\sim 25\%$ reduction in autogenous shrinkage. Also, both of these internally cured pastes showed similar shrinkage deformation to the control cement paste at w/c of 0.32, as shown in Fig. 8.

When the dosage of kraft fibers and SCF was increased to a 1% dry mass fraction, corresponding to 0.02 and 0.015 of w_e/c , respectively, SCF at a greater entrained water capacity did not exhibit any enhancement in autogenous deformation, indicating that SCF is not effective for internal curing. However, kraft fibers, both UKF and BKF, exhibited behavior similar to that of soda fibers, at the lower w_e/c as shown in Fig. 9. Since soda fibers and kraft fibers-cement pastes underwent similar autogenous deformation at equivalent fiber dosage rate (1% of dry fiber mass), the mechanical effect of

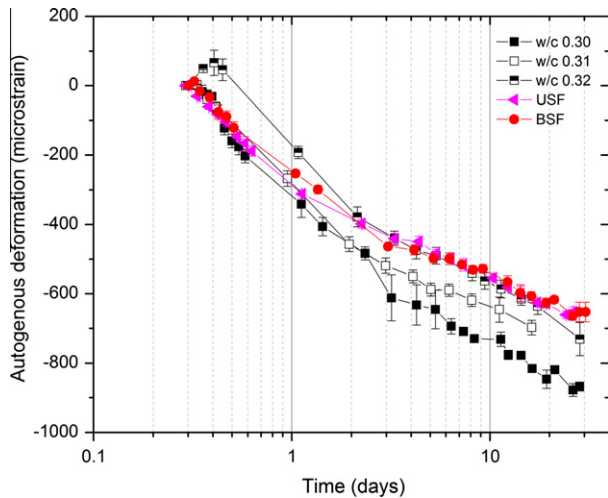


Fig. 8. Autogenous deformation of the cement pastes ($w/c = 0.30, 0.31$ and 0.32) compared with that of USF and BSF cement pastes at 0.01 of entrained water.

fibers, i.e. internal restraint, could affect the autogenous deformation of the paste. Therefore, to study the effect of the addition of fiber on the internal restraint, the autogenous shrinkage of polypropylene (PP) fiber–cement paste, where the fiber length and diameter closely approximate that of the pulp fibers but without internal curing capacity, was measured. As shown in Fig. 9, at 28 days the PP fiber–cement paste underwent autogenous strain of $-862 \pm 60 \mu\epsilon$ and exhibited no shrinkage reduction compared to the control during the entire test period. These results suggest that the inclusion of short fibers does not provide substantial internal restraint to autogenous shrinkage. Although it should be noted that the elastic modulus of wood single-fiber in a dry state is one order of magnitude greater than that of PP fiber, the elastic modulus of wood single-fiber in a wet state is also one order of magnitude lower than that in a dry state [34]. Therefore, given that the longitudinal modulus of eucalyptus kraft in a dry state is approximately 35 GPa [35], the modulus of eucalyptus fibers in a saturated state, as they would be when added to mix water and in cement paste at very early ages, would be only about 3.5 GPa. The modulus of the pulp fiber, then, is close to that of the PP fiber used for comparison. (The elastic modulus of individual wood fibers in a dry state varies from 10 to 50 GPa [36], while that of Grace

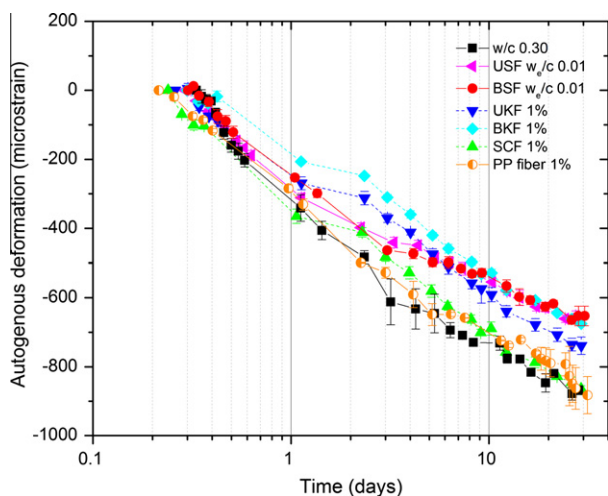
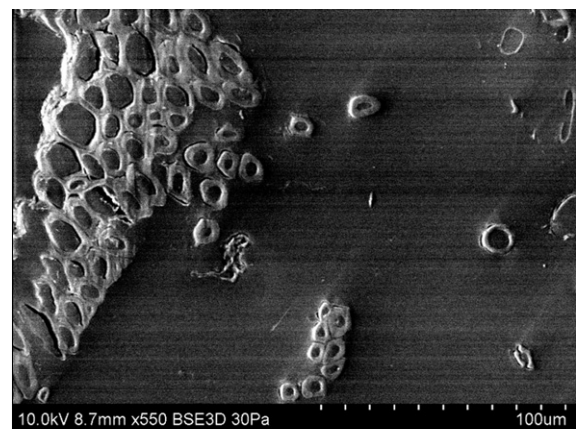


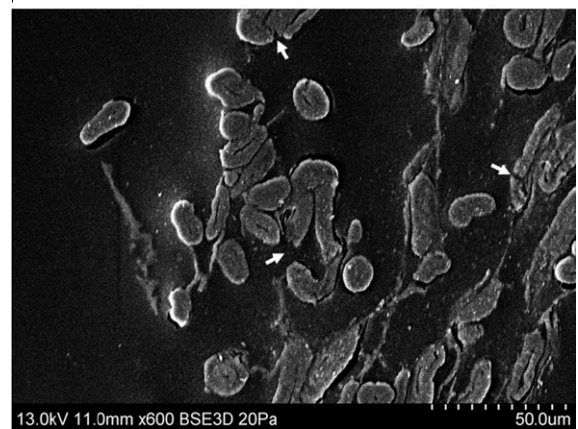
Fig. 9. Autogenous deformation of the cement paste compared with that of fiber–cement pastes at a 1% mass fraction of dry fiber.

Microfiber™ is 3.5 GPa.). This finding corresponds with a prior study which examined the efficiency of wood-derived powders and fibers for internal curing [12]. That study found that both short fibers and cellulose powder–cement pastes exhibited similar autogenous behaviors, thus they concluded that the addition of short fibers (less than 1.0 mm in length) does not provide any mechanical restraint to early age paste deformation.

Among the five fibers examined, both at the same nominal amount of entrained water and dry fiber mass percent, SCF was the least effective for internal curing and it is the only fiber subject to mechanical processing. Therefore, before discussing these results in light of the data regarding the composition and the morphology of the various fibers, it is worth examining the SCF case specifically. First, at $w_e/c = 0.01$, SCF–cement paste underwent a mere 8% reduction in autogenous shrinkage compared to control cement paste of $w/c = 0.30$. Second, the increasing dosage rate of SCF fiber to 1% dry mass fraction ($w_e/c = 0.015$) did not enhance any reduction in autogenous deformation. These behaviors were not expected, given that the SCF had the highest HR water content and a higher k than the soda fibers (which was more effective as an internal curing agent, as noted previously). The relative ineffectiveness of the SCF can be attributed to fiber bundling (or poor dispersion). Fiber bundling in SCF is related to the method of fiber processing. Since its processing is limited to partial delignification and defiberization, SCF contains fiber bundles, illustrated in Fig. 10a. Therefore, it is likely that the fibers could not be adequately dispersed. Therefore, entrained water absorbed by fibers was less likely to be well-distributed in SCF–cement paste. The correlation between dispersion and internal curing performance was



(a)



(b)

Fig. 10. SEM cross-sectional images of SCF of (a) fiber bundles and (b) fiber fracture.

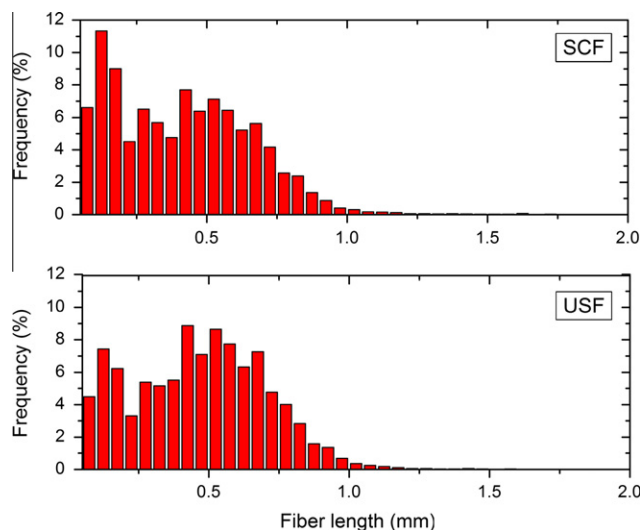


Fig. 11. Frequency distribution of percent fines content of SCF and USF observed by using FQA.

also reported in prior studies [10,37–39]. In addition to fiber bundling, the mechanical treatment in semi-chemical pulping process leads to fiber fracture, shown in Fig. 10b. This is also reflected in the higher fines content of SCF as compared to USF is shown in Fig. 11 and Table 2.

Considering in more detail the effects of fiber chemical composition and morphology, unbleached and bleached fibers from the same papermaking process, but having different ratios of cellulose-to-hemicellulose, exhibited almost the same internal curing behaviors (i.e. autogenous shrinkage behaviors and adsorption capacities). In contrast, the internal curing behaviors of fibers from different paper making process such as USF and UKF (also BSF and BKF), having similar ratios of cellulose-to-hemicellulose, were dissimilar. Together, these observations suggest that the cellulose-to-hemicellulose ratio did not significantly affect the internal curing capacity of the fibers. Although hemicellulose is the most hydrophilic constituent in wood fibers, variations in hemicellulose content could result in several and sometimes competing effects. On one hand, due to its open structure that contains many hydroxyl and acetyl groups, hemicellulose can bind relatively large amounts of water. Therefore, high water absorption is expected in fibers having high hemicellulose content. On the other hand, the removal of hemicellulose results in greater fiber cell wall porosity, increasing the amount of both mesopores and macropores. Thus, an increase in the absorption of water into fibers can also be expected as the hemicellulose content decreases [40]. (However, the removal of hemicellulose may enable greater moisture binding by the remaining cellulose. Rowell and Stout [41] state that not only hemicellulose but also accessible cellulose, both non-crystalline and the surfaces of crystalline cellulose, is crucial in moisture sorption.) The increased porosity in the cell wall may be expected to influence the rate of moisture ingress from the lumen through the cell wall, as will be discussed further.

From the results in Fig. 7, both soda fibers (USF and BSF), were more effective in mitigating autogenous shrinkage. Averaging the data from unbleached and bleached fibers (i.e., neglecting chemical composition), reductions in autogenous shrinkage of nearly 25% for the soda fibers and 7% for the kraft fibers were found compared to ordinary paste (at w/c of 0.30). These findings imply that the internal curing efficiency of these eucalyptus fibers could be related more strongly to their physical morphology than variations chemical composition of fibers. However, it should be recognized that changes in chemical composition imparted through fiber processing can influence physical structure. That is, the removal of

hemicellulose and lignin through pulping can increase cell wall porosity, which can alter the rate of moisture transport from the lumen and cell wall to the surrounding cement pastes.

Here, taking all of the data on chemical composition and morphology into account, it is proposed that the relatively better performance of the soda fibers results from their morphology. Their greater cell wall thickness is thought to contribute to their higher HR water content than kraft fibers. Therefore, the soda fibers are believed to release their entrained water into the hydrating cement during the early hydration period at a slower rate than the kraft fibers. Making entrained water available at a slightly later age is believed to improve the efficacy of hardwood fibers for internal curing.

This mechanism differs from that generally accepted for saturated lightweight aggregates and SAPs in which higher water desorption rates are believed to be more favorable [6,42]. However, since hardwood fibers are significantly smaller than lightweight aggregates and they are added at higher dosages than SAPs,¹ entrained water from well-dispersed pulp fibers is more readily available to surrounding volumes of hydrating cement. Another way of envisioning this is to imagine entrained water diffusing from internal curing sources to the surrounding pastes. In the case of pulp fibers, due to their small size (high surface area-to-volume ratio) and relatively large number, the entrained water will be made available relatively rapidly to the surrounding paste. Therefore, for the hardwood fibers examined here, it is proposed that the rates of water release from a fiber with lower HR water content might be too fast to mitigate self-desiccation, as demonstrated by data for the BKF-cement paste (Fig. 7).

And, one study on SAPs comes to a similar finding: Schroff et al. [43] reports that the SAPs that showed slow release of pore solution to the hydrating paste are more effective in mitigating autogenous shrinkage than others SAPs that desorbed pore solution too early. Overall, these findings indicate the need for further studies on a wider range of fibers and comparisons of fibers to SAPs and saturated lightweight aggregates. Such studies would examine whether thicker-walled cells in pulp fibers, especially fibers with greater HR water and lignin content, are more conducive to internal curing applications.

4. Conclusions

Results from an evaluation of the eucalyptus fiber properties and comparison with the autogenous shrinkage experimental results show a correlation between the composition and morphology of these hardwood fibers and their internal curing capacity with the following conclusions:

- Although their absorption capacity, k , was lower than kraft fibers, soda fibers with higher HR water content, exhibited better autogenous shrinkage mitigation. Therefore, the higher HR water content suggests the apparently slower rate of moisture release during early hydration, making HR water content a meaningful parameter for the assessment of, specifically, pulp fibers as internal curing agents; HR water content has not been previously examined in the context of internal curing in cement-based materials. It should be noted that HR water is a combination of both bound water and some amount of free water that are relatively difficult to remove from fiber in the drying process. The key mechanism for removing HR water is internal diffusion, which depends on fiber properties such as fiber type, pore volume, and fiber wall thickness.

¹ For internal curing application, at the same w/c , due to the lower k of pulp fibers, the dosage rate of fibers is higher than that of SAPs by about one order of magnitude.

Fig.

or these fibers, data suggests that HR water content could be related to increasing cell wall thickness, suggesting that thicker walled fibers could be more suitable for internal curing.

- The open lumens of fractured fibers seem to limit the ability of fiber to hold water resulting in less effectiveness of internal curing, as observed in SCF case.
- Confirming observations in other research, the dispersability of the internal curing agent was found to affect the fiber's capacity for mitigating autogenous shrinkage. Because of the partial delignification and partial defiberization of SCF, these fibers were poorly dispersed in the cement paste. Therefore, SCF could not provide a sufficient amount of entrained water throughout the paste, resulting in low internal curing capability.
- In contrast to soda fibers, SCF fiber with high HR water content was not effective as an internal curing agent because of its unsuitable physical morphology, indicating that the physical morphology of fibers is crucial and therefore is a factor which should be taken into account when using pulp fibers as internal curing agents.
- Due to their small size and large number, with adequate dispersion of a fiber, entrained water is more readily released into the surrounding volume of hydrating cement paste. Therefore, the mechanism controlling efficiency of pulp fibers for internal curing differs from that of saturated lightweight aggregates. For lightweight aggregates, the higher desorption rate is favorable. For hardwood pulp fibers, however, a slower moisture release rate appears to be more favorable for internal curing.
- Comparing between the effects of fiber chemical composition and morphology, results presented in the paper indicate that the internal curing efficiency of Eucalyptus fibers is related more strongly to their physical morphology than variations in chemical composition. However, further studies on lignin-rich fibers are needed to verify these findings across a wider range of fiber compositions.

Acknowledgements

The authors gratefully acknowledged SCG cement for the financial support and Dr. Andrea Mezencevova for her assistance in autogenous shrinkage experiments.

References

- [1] Bentz DP, Weiss WJ. Internal curing: a 2010 state-of-the art review. National Institute of Standards and Technology; 2011.
- [2] El-Dieb AS. Self-curing concrete: water retention, hydration and moisture transport. *Constr Build Mater* 2007;21(6):1282–7.
- [3] Jensen OM, Hansen PF. Water-entrained cement-based materials I. Principles and theoretical background. *Cem Concr Res* 2001;31(4):647–54.
- [4] Jensen OM, Hansen PF. Water-entrained cement-based materials II. Experimental observations. *Cem Concr Res* 2002;32(6):973–8.
- [5] Bentur A, Igarashi S, Kovler K. Prevention of autogenous shrinkage in high-strength concrete by internal curing using wet lightweight aggregates. *Cem Concr Res* 2001;31(11):1587–91.
- [6] Zhutovsky S, Kovler K, Bentur A. Revisiting the protected paste volume concept for internal curing of high-strength concretes. *Cem Concr Res* 2011;41(9):981–6.
- [7] Philleo R. Concrete science and reality. In: Skalny J, Mindess S, editors. *Materials science of concrete II*. Westerville, OH: American Ceramic Society; 1991. p. 1–8.
- [8] Siramanont J, Vichit-Vadakan W, Siriwatwechakul W. The impact of SAP structure on the effectiveness of internal curing. In: International RILEM conference on use of superabsorbent polymers and other new additives in concrete. Denmark: RILEM; 2010.
- [9] Siriwatwechakul W, Siramanont J, Vichit-Vadakan W. Superabsorbent polymer structures. In: International RILEM conference on use of superabsorbent polymers and other new additives in concrete. Denmark: RILEM; 2010.
- [10] Kawashima S, Shah SP. Early-age autogenous and drying shrinkage behavior of cellulose fiber-reinforced cementitious materials. *Cem Concr Compos* 2011;33(2):201–8.
- [11] Mezencevova A, Garas V, Nanko H, Kurtis K. Influence of thermomechanical pulp fiber compositions on internal curing of cementitious materials. *J Mater Civ Eng* 2012;24(8):970–5.
- [12] Mohr BJ, Premenko L, Nanko H, Kurtis KE. Examination of wood-derived powder and fibers for internal curing of cement-based materials. In: Persson B, Bentz D, Nilsson LO, editors. *Proceedings of the 4th international seminar on self-desiccation and its importance in concrete technology*. Gaithersburg, MD; 2005. p. 229–44.
- [13] Tonoli GHD, Savastano H, Fuente E, Negro C, Blanco A, Lahr FAR. Eucalyptus pulp fibres as alternative reinforcement to engineered cement-based composites. *Ind Crop Prod* 2010;31(2):225–32.
- [14] Chinga-Carrasco G, Lenes M, Johnsen PO, Hult EL. Computer-assisted scanning electron microscopy of wood pulp fibres: dimensions and spatial distributions in a polypropylene composite. *Micron* 2009;40(7):761–8.
- [15] Reme PA, Johnsen PO, Helle T. Assessment of fibre transverse dimensions using SEM and image analysis. *J Pulp Pap Sci* 2002;28(4):122–8.
- [16] Laine J, Stenius P, Carlsson G, Strom G. Surface characterization of unbleached kraft pulps by means of ESCA. *Cellulose* 1994;1(2):145–60.
- [17] Yang H, Yang R, Chen H, Lee DH, Zheng C. Characteristic of hemicellulose, cellulose and lignin pyrolysis. *Fuel* 2007;86(12–13):1781–8.
- [18] Park S, Venditti RA, Jameel H, Pawlak JJ. Hard to remove water in cellulose fibers characterized by high resolution thermogravimetric analysis – methods development. *Cellulose* 2006;13(1):23–30.
- [19] Smook GA. *Handbook of pulp and paper technologists*. Atlanta, GA: TAPPI; 1982.
- [20] Johansen NA, Millard MJ, Mezencevova A, Garas VY, Kurtis KE. New method for determination of absorption capacity of internal curing agents. *Cem Concr Res* 2009;39(1):65–8.
- [21] ASTM D4442-07. Standard test methods for direct moisture content measurement of wood and wood-base materials. West Conshohocken (PA): ASTM international; 2007.
- [22] ASTM C1698-09. Standard Test method for autogenous strain of cement paste and mortar. West Conshohocken (PA): ASTM international; 2010.
- [23] ASTM C191-08. Standard test methods for time of setting of hydraulic cement by vicat needle. West Conshohocken (PA): ASTM international; 2008.
- [24] JdA Clark. *Pulp technology and treatment for paper*. San Francisco: Miller Freeman Publications; 1985.
- [25] Ramezani O, Nazhad MM. The effect of coarseness on paper formation. <http://www.tappsa.co.za/archive2/APPW_2004/Title2004> [accessed in June 2012].
- [26] Paavilainen L. Fiber structure. In: Mark RE, Habeger CC, Borch J, Lyne MB, editors. *Handbook of physical testing of paper*. New York: Marcel Dekker, Inc.; 2002. p. 700–25.
- [27] Dutt D, Tyagi CH. Comparison of various eucalyptus species for their morphological, chemical, pulp and paper making characteristics. *Indian J Chem Technol* 2011;18(2):145–51.
- [28] Pulkkinen I, Alopaeus V, Fiskari J, Joutsimo O. The use of fibre wall thickness data to predict handsheet properties of eucalypt pulp fibres. *O Papel: ABCTP*; 2008. p. 71–85.
- [29] Park S, Venditti RA, Jameel H, Pawlak JJ. A novel method to evaluate fibre hornification by high resolution thermogravimetric analysis. *Appita J* 2006;59(6):481–5.
- [30] Stone JE, Scallan AM. The effect of component removal upon the porous structure of the cell wall of wood. II. Swelling in water and the fiber saturation point. *Tappi J* 1967;50(10):496–501.
- [31] Goring DAL. A speculative picture of the delignification process. *ACS Symposium Series*. Washington, DC: American Chemical Society; 1977. p. 273–7.
- [32] Odler I, Becker T. Effect of some liquefying agents on properties and hydration of portland-cement and tricalcium silicate pastes. *Cem Concr Res* 1980;10(3):321–31.
- [33] Mohr BJ, Hood KL. Influence of bleed water reabsorption on cement paste autogenous deformation. *Cem Concr Res* 2010;40(2):220–5.
- [34] Coutts RSP. Wood fibres in inorganic matrices. *Chem Aust* 1983;50:143–8.
- [35] Neagu RC, Gamstedt EK, Berthold F. Stiffness contribution of various wood fibers to composite materials. *J Compos Mater* 2006;40(8):663–99.
- [36] Hamad W. *Cellulosic materials: fibers, networks, and composites*. Boston, MA: Kluwer Academic Publishers; 2002.
- [37] Akcay B, Tasdemir MA. Effects of distribution of lightweight aggregates on internal curing of concrete. *Cem Concr Compos* 2010;32(8):611–6.
- [38] Geiker M, Bentz DP, Jensen OM. Mitigating autogenous shrinkage by internal curing. In: Ries JP, Holm TA, editors. *American Concrete Institute Special Publication 218, High Performance Structural Lightweight, Concrete* 2004. p. 143–54.
- [39] Bentz DP, Snyder KA. Protected paste volume in concrete – extension to internal curing using saturated lightweight fine aggregate. *Cem Concr Res* 1999;29(11):1863–7.
- [40] Wan JQ, Wang Y, Xiao Q. Effects of hemicellulose removal on cellulose fiber structure and recycling characteristics of eucalyptus pulp. *Bioresour Technol* 2010;101(12):4577–83.
- [41] Rowell RM, Stout HP. Jute and kenaf. In: Lewin M, editor. *Handbook of fiber chemistry*. Marcel Dekker; 1998. 1103p.
- [42] Castro J, Keiser L, Golias M, Weiss J. Absorption and desorption properties of fine lightweight aggregate for application to internally cured concrete mixtures. *Cem Concr Compos* 2011;33(10):1001–8.